A Novel Method for Characterizing Beam Hardening Artifacts in Cone-beam Computed Tomographic Images

Aaron Fox, DDS, Bettina Basrani, DDS, PhD, FRCD(C),* Anil Kishen, BDS, MDS, PhD,* and Ernest W.N. Lam, DMD, MSc, PhD, FRCD(C)†*

Abstract

Introduction: The beam hardening (BH) artifact produced by root filling materials in cone-beam computed tomographic (CBCT) images is influenced by their radiologic K absorption edge values. The purpose of this study was to describe a novel technique to characterize BH artifacts in CBCT images produced by 3 root canal filling materials and to evaluate the effects of a zirconium (Zr)-based root filling material with a lower K edge (17.99 keV) on the production of BH artifacts. **Methods:** The palatal root canals of 3 phantom model teeth were prepared and root filled with gutta-percha (GP), a Zr root filling material, and calcium hydroxide paste. Each phantom tooth was individually imaged using the CS 9000 CBCT unit (Carestream, Atlanta, GA). The "light" and "dark" components of the BH artifacts were quantified separately using ImageJ software (National Institutes of Health, Bethesda, MD) in 3 regions of the root. Mixed-design analysis of variance was used to evaluate differences in the artifact area for the light and dark elements of the BH artifacts. **Results:** A statistically significant difference in the area of the dark portion of the BH artifact was found between all fill materials and in all regions of the phantom tooth root ($P < .05$). GP generated a significantly greater dark but not light artifact area compared with Zr ($P < .05$). Moreover, statistically significant differences between the areas of both the light and dark artifacts were observed within all regions of the tooth root, with the greatest artifact being generated in the coronal third of the root ($P < .001$). **Conclusions:** Root canal filling materials with lower K edge material properties reduce BH artifacts along the entire length of the root canal and reduce the contribution of the dark artifact. *(J Endod 2018;44:869–874)*

Key Words

Beam hardening artifact, CBCT, cone beam computed tomography, dark artifact, gutta-percha, light artifact, zirconium

Significance

A novel method was developed to characterize and quantify the beam hardening artifact arising from CBCT imaging. A zirconium-based root filling produced significantly greater artifact reduction along the length of the root compared with gutta-percha.

Recently, high-resolution, limited field of view cone-beam computed tomographic (CBCT) imaging has been used to evaluate teeth in clinical endodontics (1). CBCT imaging provides 3-dimensional information that has been shown to increase the reliability of decision making for diagnosis and treatment planning compared with 2-dimensional radiography (2, 3). Unfortunately, teeth that have undergone endodontic and/or restorative procedures with highly attenuating materials such as gutta-percha (GP), metal posts, and crowns are prone to display CBCT image artifacts that can potentially mask abnormalities (4).

Artifacts produced in radiographic imaging represent a discrepancy between the attenuation features of the actual physical object under investigation and the reconstructed image (5). Several artifacts have been reported with CBCT imaging that degrade the image quality. One of these that is commonly encountered is the beam hardening (BH) artifact (6).

A BH artifact occurs when lower-energy photons in the polychromatic x-ray beam are absorbed by a higher-attenuating or radiopaque material in preference to higher-energy photons. The attenuated x-ray beam exits this material with a higher mean energy than the incident or primary beam (ie, it becomes "harder" or more "intense") when it reaches the detector. This results in distortion of the attenuated x-ray beam because of differential absorption by the material (otherwise known as the "cupping" artifact) and produces streaks and dark bands on the image (Fig. 1*A* and *B*) (7). BH artifacts degrade image quality and compromise the diagnostic value of the image, rendering the image difficult to interpret and making the process a time-consuming one (8, 9). Understanding the characteristic features of BH artifacts may enable us to develop novel strategies to extract critical diagnostic information from the image (9).

Modern GP is composed of inorganic components such as zinc oxide and barium sulfate, and the proportions of these compounds contribute to the radiopacity of the material (10). Recently, EndoTechnologies LLC (Shrewsbury, MA) produced a root filling material with a central core comprised of a zirconium (Zr) particle suspension, thereby imparting different radiologic properties compared with conventional GP. The Zr atom enables greater transmission of the x-ray beam through the material because of its lower K absorption edge (17.99 keV), and compared with barium, Zr is a weaker radiologic attenuator for the mean energy of the polychromatic x-ray

From the Graduate Programs in *Endodontics and †Oral and Maxillofacial Radiology, Faculty of Dentistry, The University of Toronto, Toronto, Ontario, Canada.
Address requests for reprints to Dr Aaron Fox, Graduate Programs in Endodontics, Faculty of Dentistry, The University of Toronto, 124 Edward Street, Toronto, ON M5G 1G6, Canada. E-mail address: aafox1@gmail.com
0099-2399/$ - see front matter

https://doi.org/10.1016/j.joen.2018.02.005

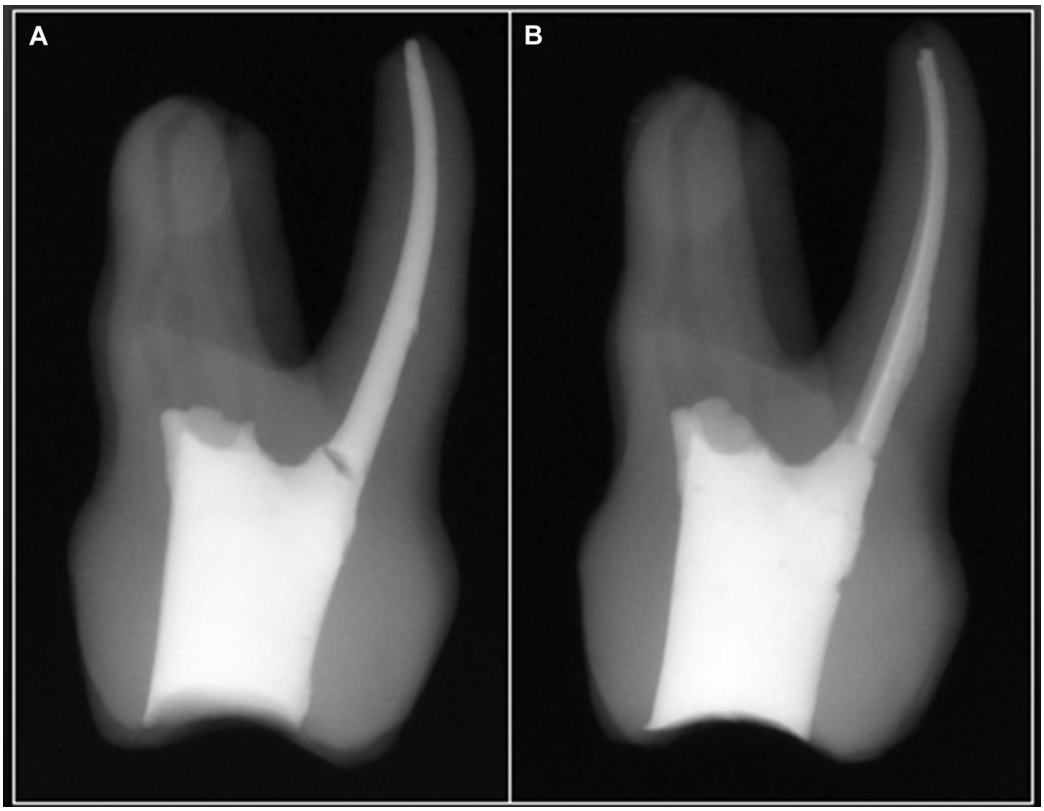

Figure 1. Two-dimensional periapical image of a phantom tooth palatal canal root filling. (*A*) GP single-cone with BC Sealer. (*B*) Zr single cone with BC Sealer.

beam (approximately 33 keV) (9). Because the barium atom in barium sulfate of GP has a higher K edge (37.4 keV) than Zr and given that this value is closer to the mean intraoral x-ray beam energy, the barium atom preferentially absorbs the x-ray beam energy compared with Zr (11). On the basis of these differences in x-ray absorption characteristics, we hypothesize that Zr should be associated with less BH artifacts than GP. Furthermore, the reduction in artifact production from Zr on CBCT images may enable more accurate and reliable interpretation of images of endodontically treated teeth. The aim of this study was to develop a reproducible methodology for characterizing BH artifacts from CBCT images and to determine if Zr can reduce BH artifacts over GP in an experimental model.

Methods

The palatal root canals of 4 preaccessed standardized maxillary molar phantom teeth (Dentalike; Dentsply Sirona, Tulsa, OK) were used. The optical features of a phantom tooth model are 27% that of dentin (% aluminum equivalent) (12). The palatal canals of the teeth were initially negotiated, and patency was confirmed with a 10 K-Flexofile (Tulsa Dentsply Sirona, Tulsa, OK); after which, rotary instruments (Vortex, Tulsa Dentsply Sirona) were used according to the manufacturer's instructions to prepare canals up to a 45.06 master file. Patency was maintained, and the canal was irrigated with 2% sodium hypochlorite (Clorox Company, Oakland, CA) between the introduction of each instrument. A 45.06 master GP cone (Vortex GP, Tulsa Dentsply Sirona) and a 45.06 master Zr point (EndoTechnologies LLC, Shrewsbury, MA) were fitted to produce tug back 0.5 mm short of the working length. A light application of EndoSequence BC Sealer (Brasseler, Savannah, GA) was applied to the tip of each master cone, and the cones were cut flush to the level of the palatal canal orifice and placed into the canal using the single-cone technique. A third model tooth was filled with calcium hydroxide (Pulpdent Paste; Pulpdent Corp, Waterdown, MA) to the working length of the palatal canal. The palatal canal in a fourth phantom tooth was left untreated (control). All orifices were sealed with a thin layer of composite resin (Filtek Bulk; 3M ESPE, St Paul, MN) and filled to the occlusal surface.

A CS 7600 photostimulable phosphor plate (Carestream Dental, Atlanta, GA) was used to make periapical images to confirm that root filling material was well adapted to the root canal walls in the buccolingual and mesiodistal dimensions. Images were exposed using a dental x-ray unit (Gendex GX-770; Gendex Dental Systems, Hatfield, PA) at 70 kVp and 10 mA (Fig. 1*A* and *B*).

A reproducible jig was constructed using polyvinyl siloxane impression material (President; Coltene/Whaledent AG, Alstatten, Switzerland) and was used to establish an index to position the occlusal surface of the phantom tooth to the base of a disposable paper cup (Fig. 2*A* and *B*). The cup was placed on a chin rest using a wax jig so that the exact position of the paper cup and phantom tooth could be reproducibly positioned with the CS 9000 3D CBCT system (Carestream Dental). Exposure parameters were optimized for the phantom teeth, which were imaged at 76-μm voxel size resolution using a 5 cm (diameter) $\times$ 3.7 cm field of view.

Artifact Measurement

CBCT volumes were uploaded into CS 3D viewing software (Carestream Dental), and the palatal root canal of each phantom tooth was aligned and then measured in the coronal plane. The palatal root was divided into 3 equal lengths: the coronal, middle, and apical thirds. A midpoint axial within each third of the root was established for all samples, and 2 additional regions were

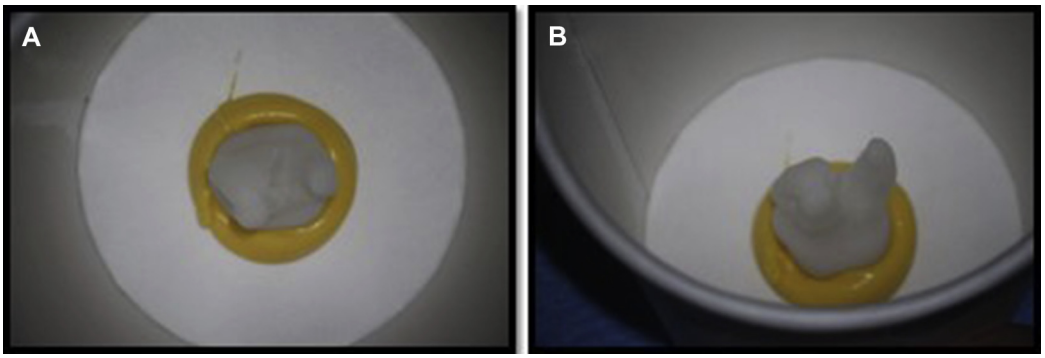

Figure 2. Phantom tooth model jig apparatus with polyvinyl siloxane impression material index. (*A*) Bird's-eye view of the phantom tooth. (*B*) Long-axis view of the phantom tooth.

identified 1 mm apical and 1 mm coronal to this midpoint (Fig. 3*A*–*D*). A total of 9 measurements were made through the entire length of each palatal root. Each axial root image was individually uploaded into ImageJ software (National Institutes of Health, Bethesda, MD). The axial images from the no fill (control) group were used to establish baseline pixel intensity values for the phantom tooth. The highest (ie, lightest) pixel intensity value of the phantom tooth was 149.0 ± 0.5 arbitrary units, and the lowest (darkest) background pixel intensity value was 27.0 ± 0.2. The pixel intensity values for all root filling materials were 255.0 ± 0.0 (Fig. 4*A* and *B*).

Using these values, the artifact pixel intensity value ranges were established for "light" and "dark" artifacts as follows. The light artifact value range was defined as ranging from 149.0 ± 0.5 to 254.9, and the dark artifact value range was defined as ranging from 0.0 to 27.0 ± 0.2. A color threshold overlay tool was used to represent the area for light and dark artifacts for each axial section, and a precalibrated region of interest measurement tool was used to establish the area measurements for each axial section (Fig. 5*A*–*C*).

Statistical Analysis

Data normality was confirmed using Kolmogorov-Smirnov and Shapiro-Wilk tests. Mixed-design analysis of variance was used to evaluate differences between 4 root canal filler groups (ie, no fill, calcium hydroxide, GP, and Zr) and the difference between 3 regions of the tooth root (coronal, middle, and apical thirds) for both the light and dark artifacts. All inferential analyses were conducted using IBM SPSS software (SPSS Version 24; IBM Corp, Armonk, NY). The null hypothesis was rejected when P was <.05.

Results

The amount of light artifacts between GP and calcium hydroxide paste exhibited a statistically significant difference (P = .001). The GP root filling material showed the greatest overall light area compared with Zr, calcium hydroxide paste, and the control; however, the difference between the light areas produced by the GP root filling and Zr root filling materials was not statistically significant (P = .079). However, a statistically significant difference was found between the area of the light artifact in the 3 root regions (P < .001), with the greatest amount of light artifact in the coronal thirds of each root.

A statistically significant difference was found for the amount of dark artifact between all groups (P < .001). The GP root filling material showed significantly larger areas for dark artifact compared with Zr root filling material (P = .04).

Statistically significant differences were found between all 3 root regions for both GP and Zr (P < .001). These findings are summarized in Figure 6*A* and *B*.

Discussion

The current study has developed a novel approach to quantify BH artifacts into 2 base components: light and dark artifacts. Our decision to use the phantom tooth model instead of an extracted tooth for these experiments is important because of the unique optical features of the phantom tooth model (27% aluminum equivalent). The model tooth absorbs less of the polychromatic x-ray beam than tooth tissue would, thus enabling a truer representation of the attenuating effects of the root filling materials themselves without the additional contribution of (primarily) root dentin. Furthermore, production of the tooth model as well as its morphology is standardized and reproducible, reducing the possibility that dentin wall thickness variability that may be found between different natural teeth might heterogeneously attenuate the incident x-ray beam. Although this *in vitro* model may have some limitations, we do believe that the standardized tooth model offers many advantages that cannot be obtained using natural teeth in a study such as this. Moreover, we believe this model has allowed us to validate what we believe to

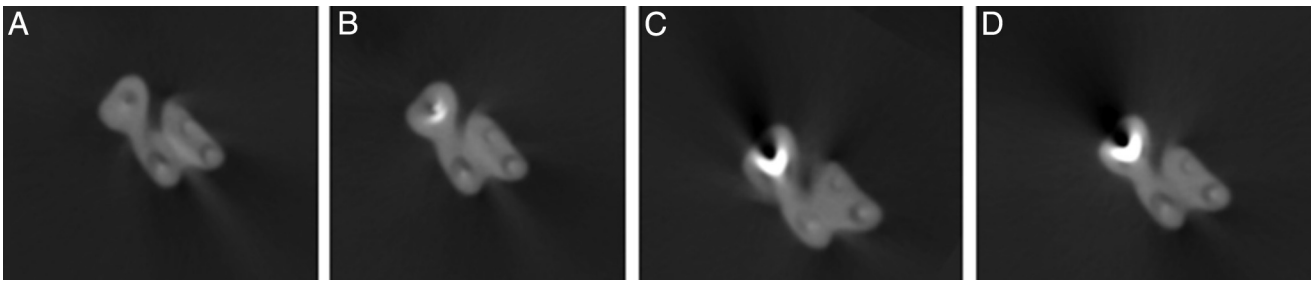

Figure 3. Mid-coronal CBCT axial section of (*A*) no-fill (negative control), (*B*) calcium hydroxide paste, (*C*) Zr, and (*D*) GP.

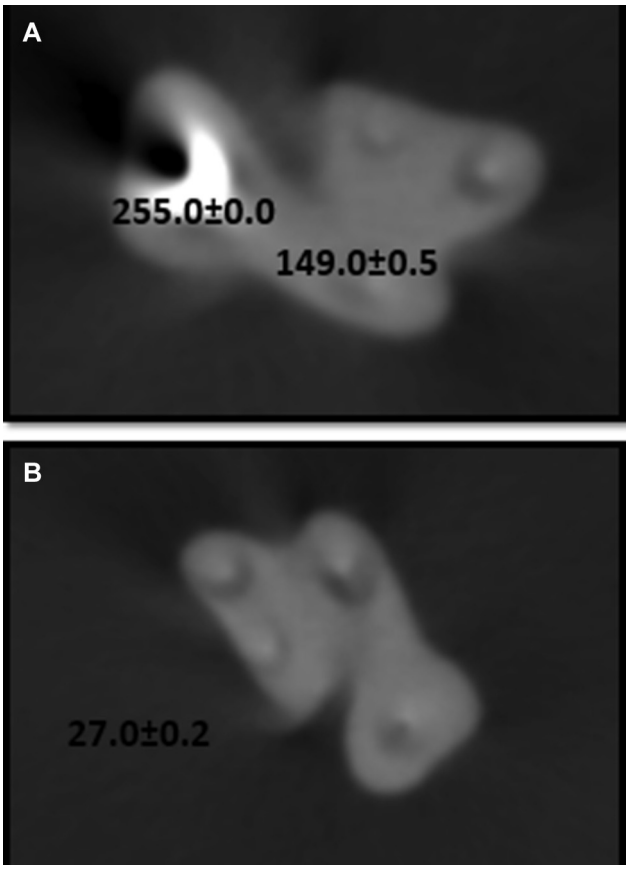

Figure 4. (*A*) Light artifact pixel intensity range. Use of the GP sample (coronal section) to establish parameters for the light artifact pixel intensity range. The base density of the phantom tooth was determined to be 149.0 ± 0.5, and the base density value of the root filling materials (GP and Zr) were determined to be 255.0 ± 0.0. (*B*) Dark artifact pixel intensity range. Use of the no fill (negative control, coronal section) to establish the darkest pixel intensity value of the background was determined to be 27.0 ± 0.2.

be an extremely novel and innovative technique for quantifying BH artifacts, something that has never before been done.

The light and dark components of BH artifacts are commonly observed in CBCT imaging of teeth treated with root canal filling materials. Previous studies have only qualitatively classified the imaging features of BH artifacts as "cupping effects," "hypodense halos," and dark streaks and bands (6, 7, 13). Although the area measurements of the light artifact for GP and Zr were not statistically significant ($P > .05$), the area of the GP-generated light artifact was, not surprisingly, greater than for canals filled with calcium hydroxide ($P = .001$) or left unfilled ($P < .001$). Interestingly, the area of the light artifact varied with the region of the canal; a greater light artifact area was associated with the coronal portion of the filled canal ($P < .001$). This may be caused by the larger volume or cross-sectional area of the material in the coronal third of the root. With tapering of the prepared canal and the amount of material in the middle and apical thirds of the canal, less light artifact is observed.

Among the most obvious CBCT artifacts associated with BH is the dark artifact, the so-called dark bands and hypodense regions observed adjacent to the radiopaque material (6, 9). The dark artifact areas of BH are the result of a discrepancy in the algorithmic processing of the imaging information from the detector. The detector assumes the primary x-ray beam exiting the tube head is monochromatic, therefore assigning incorrectly lower grayscale values in the back-projection process. This results in the reconstruction of an image with characteristic dark areas (5, 9). The features of a dark artifact extend well beyond the root surface and obscure the perimeter of the external phantom root surface. GP showed a significantly larger dark artifact area measurement than the other materials ($P < .001$). In particular, the differences between the dark artifact area of GP compared with the Zr material were statistically significant ($P < .05$) (for calcium hydroxide and unfilled canals, $P < .001$). As with the light artifact, there were statistically significant regional effects within each third of the root ($P < .001$).

GP is the most widely used root canal obturating material because it generally satisfies the necessary biological, mechanical, and technical requirements (14). Although GP is easily discernable on a conventional intraoral image, it generates substantial imaging artifacts degrading the quality of the CBCT image. The radiologic properties of GP that contribute to its radiopacity are related to the proportions of inorganic filler containing zinc and barium. These radiologic features are intended to satisfy ISO requirements for radiopacity of an endodontic filling material, which specifies greater than 3 mm equivalent of aluminum (15).

Recently, the American Association of Endodontists and the American Academy of Oral and Maxillofacial Radiology established a joint position statement on the use of CBCT imaging as the imaging modality of choice in endodontics (1). These recommendations specify common clinical scenarios in which CBCT imaging is indicated as a tool to improve diagnostic efficacy. For this reason, reports continue to show the emerging trend in the use of CBCT systems in clinical endodontics (2). However, the presence of artifacts can severely compromise image quality by reducing contrast, obscuring structures, and limiting the diagnostic value within areas of interest, making interpretation difficult and time-consuming (7). For this reason, several methods have been examined to reduce imaging artifacts to improve diagnostic capability. One such application is the use of artifact reduction (AR) software in which proprietary algorithms appear to reduce the effects of BH. However, it has been shown by previous *in vitro* studies that AR software did not lead to a more accurate diagnosis in the detection of simulated root fractures (13, 16, 17). Previous studies have also reported that in the presence of GP, AR software negatively alters the image by improperly reducing the artifact, removing peripheral GP from the image, and producing secondary artifacts (17).

Increasing exposure parameters such as tube voltage (kVp) and/or filament current (mA) has been suggested as a means for reducing artifact formation and enhancing image quality (18). The increased radiation dose from doing this is not reflected by an improvement in diagnosis (19). One such study found that the degradation of the image because of BH artifacts was so extensive that the imaging mode had no influence on the diagnostic ability (8).

The current study has described a novel method for quantifying BH artifacts from CBCT imaging and the influence of root filling material properties on the radiologic effects of BH artifact production. We chose to use a Zr root filling material because of its inner-core suspension of Zr particles, which contributes a more favorable (ie, lower) radiologic property compared with the higher K edge of conventional GP. Zr fill reduced artifact area measurements, in particular for the dark artifact along the entire length of the phantom root. Overall, dark artifact feature area reductions between GP and Zr were found to be inversely proportional to the diameter of the root filling such that smaller artifact area reductions were observed in the coronal and middle regions of the phantom root (32.6% and 32.2% area reduction) compared with the apical region (51.6% area reduction. For calcium hydroxide, the dark artifact area approached 0 (no artifact). This is also related to the increased thickness associated with the taper of the root filling material from apical to coronal. Minimizing image compromising features

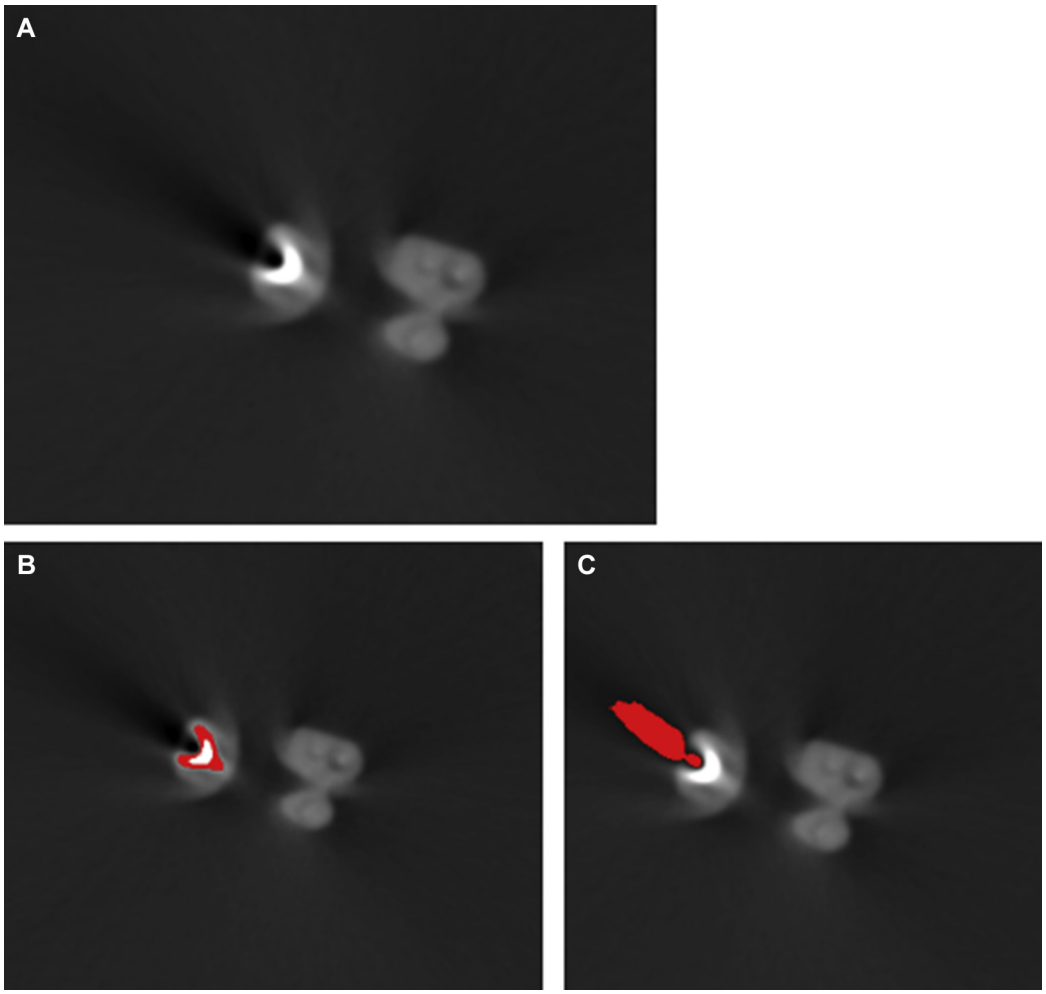

Figure 5. (*A*) Axial section through a zirconium-treated root. (*B*) Axial section through a zirconium-treated root showing light artifact color threshold overlay corresponding to the pixel intensity range established in Figure 4*A*. Color threshold overlay of light artifact pixel intensity value range. (*C*) Axial section through a zirconium-treated root showing dark artifact color threshold overlay corresponding to the pixel intensity range established in Figure 4*B*.

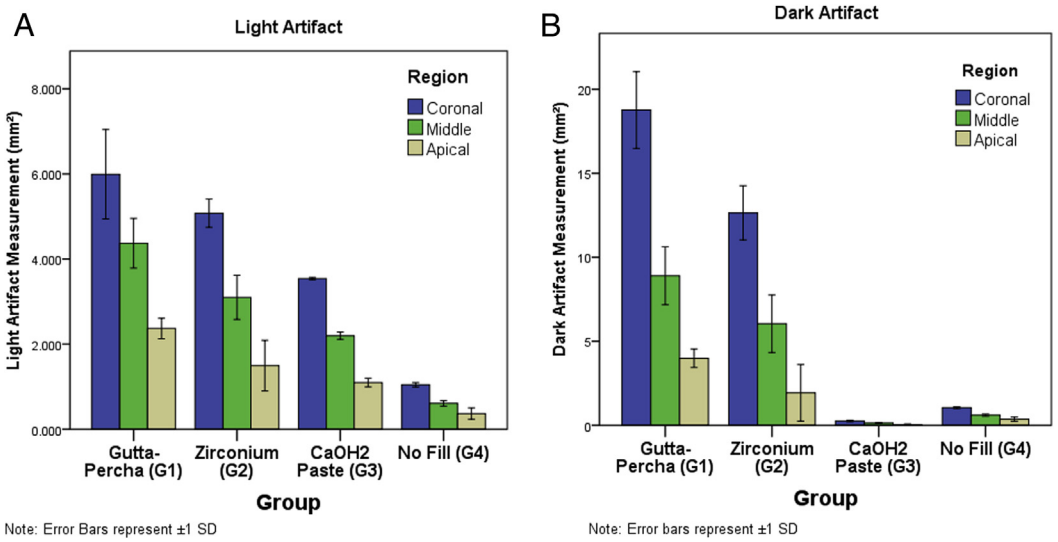

Figure 6. (*A*) The areas of the light artifacts between GP, Zr, calcium hydroxide, and no fill within 3 regions of each phantom tooth root (mm^2). (*B*) The areas of the dark artifacts between GP, Zr, calcium hydroxide, and no fill within 3 regions of each phantom tooth root (mm^2).

of artifacts to that magnitude along the length of the root system may prove to add diagnostic efficacy in specific clinical scenarios, such as root fracture detection, which tend to propagate from the apical root region to the coronal region.

Conclusion

Root canal filling materials with reduced K edge radiologic properties can reduce the impact of BH artifacts. A phantom tooth model system used in conjunction with different root filling materials accurately depicted the characteristic features of BH artifacts. Alternative material properties of root filling materials that influence radiologic features should be considered for additional research and clinical use in the age of CBCT imaging in endodontics.

Acknowledgments

The authors are grateful to the Oral and Maxillofacial Radiology Clinic at the University of Toronto (Toronto, Canada) for its support of the study.

Supported by the Alpha Omega Foundation, the Canadian Academy of Endodontics Foundation, and the Dr. Lloyd and Mrs. Kay Chapman Chair in Clinical Science.

The authors deny any conflicts of interest related to this study.

References

1. *AAE and AAOMR Joint Position Statement: Use of Cone Beam Computed Tomography Imaging in Endodontics - 2015/2016 Update*. Chicago: American Association of Endodontists; 2015.
2. Setzer FC, Hinckley N, Kohli MR, Karabucak B. A survey of cone-beam computed tomographic use among endodontic practitioners in the United States. J Endod 2017;43:699–704.
3. Rosen E, Taschieri S, Del Fabbro M, et al. The diagnostic efficacy of cone-beam computed tomography in endodontics: a systematic review and analysis by a hierarchical model of efficacy. J Endod 2015;41:1008–14.
4. Bernardes RA, de Moraes IG, Hungaro Duarte MA, et al. Use of cone-beam volumetric tomography in the diagnosis of root fractures. Oral Surg Oral Med Oral Pathol Oral Radiol Endod 2009;108:270–7.
5. Schulze RK, Berndt D, d'Hoedt B. On cone-beam computed tomography artifacts induced by titanium implants. Clin Oral Implants Res 2010;21:100–7.
6. Schulze R, Heil U, Gross D, et al. Artefacts in CBCT: a review. Dentomaxillofac Radiol 2011;40:265–73.
7. Barrett JF, Keat N. Artifacts in CT: recognition and avoidance. Radiographics 2004; 24:1679–91.
8. Neves FS, Freitas DQ, Campos PS, et al. Evaluation of cone-beam computed tomography in the diagnosis of vertical root fractures: the influence of imaging modes and root canal materials. J Endod 2014;40:1530–6.
9. Makins SR. Artifacts interfering with interpretation of cone beam computed tomography images. Dent Clin North Am 2014;58:485–95.
10. Maniglia-Ferreira C, Gurgel-Filho ED, de Araujo Silva JB Jr, et al. Chemical composition and thermal behavior of five brands of thermoplasticized gutta-percha. Eur J Dent 2013;7:201–6.
11. Curry TSI, Dowdey JE, Murray RC Jr. *Christensen's Introduction to the Physics of Diagnostic Radiology*, 3rd ed. Philadelphia: Lea & Febiger; 1984.
12. Dentalike. Available at: www.dentalike.net. Accessed July 30, 2017.
13. Vasconcelos KF, Nicolielo LF, Nascimento MC, et al. Artefact expression associated with several cone-beam computed tomographic machines when imaging root filled teeth. Int Endod J 2015;48:994–1000.
14. Chandra BS, Gopikrishna V. *Grossman's Endodontic Practice 13th Edition*. New Dehli, India: Wolters Kluwer; 2014.
15. International Standards Organization. ISO 6876. *Dental root canal sealing materials*. Geneva, Switzerland: International Standards Organization; 2001.
16. de Rezende Barbosa GL, Sousa Melo SL, Alencar PN, et al. Performance of an artefact reduction algorithm in the diagnosis of *in vitro* vertical root fracture in four different root filling conditions on CBCT images. Int Endod J 2016;49: 500–8.
17. Bechara B, Alex McMahan C, Moore WS, et al. Cone beam CT scans with and without artefact reduction in root fracture detection of endodontically treated teeth. Dentomaxillofac Radiol 2013;42:20120245.
18. Pauwels R, Stamatakis H, Bosmans H, et al. Quantification of metal artifacts on cone beam computed tomography images. Clin Oral Implants Res 2013;24(Suppl A100): 94–9.
19. Pinto MG, Rabelo KA, Sousa Melo SL, et al. Influence of exposure parameters on the detection of simulated root fractures in the presence of various intracanal materials. Int Endod J 2017;50:586–94.